Hydrogen Generation

DOI: 10.1002/ange.201304652

Highly Efficient Dehydrogenation of Formic Acid over a Palladium-Nanoparticle-Based Mott–Schottky Photocatalyst**

Yi-Yu Cai, Xin-Hao Li, Ya-Nan Zhang, Xiao Wei, Kai-Xue Wang, and Jie-Sheng Chen**

The high energy density of formic acid (FA) along with its low toxicity, low cost, and high stability make it a promising hydrogen carrier for safe hydrogen storage and hydrogen-based green-energy applications.[1–8] FA has been obtained in large quantities by the hydrogenation of waste carbon dioxide from industry, biomass processing, and artificial photosynthesis.[1] Thus, the catalytic dehydrogenation of FA with the release of hydrogen gas under mild conditions can meet the increasing demand for alternative technologies for the generation of hydrogen in a more sustainable manner. The development of efficient catalysts remains the main hurdle for practical applications of this approach. The dehydrogenation of FA can be catalyzed by homogeneous metal complexes or clusters with high hydrogen-evolution rates by the addition of a base and/or organic ligands.[2,8] Alternatively, heterogeneous catalysts based on metal nanoparticles may be used. Such catalysts are generally more recyclable and stable but less active than their homogeneous counterparts. The ideal sustainable catalyst should be recyclable, inexpensive, and efficient for the dehydrogenation of FA in pure water or without a solvent in the absence of any other additives at ambient temperature.

In the past, much effort has been focused on the improvement of catalysts based on palladium nanoparticles (Pd NPs).[3–7] Pd NPs are the most active single-component nanocatalysts reported so far and have the lowest effective barrier for the dehydrogenation of FA without additives.[4] Recently, there have been many attempts to rationally design bimetallic[5] and trimetallic[6] nanoparticles with controlled sizes, core–shell structures,[7] and/or optimized content of alloying metals. Some of the bimetallic and trimetallic catalysts exhibited much higher initial turnover frequencies (TOFs) at relatively low temperatures. However, their fabrication processes were rather complicated, which limited their further practical application. Approaches for the significant enhancement of the room-temperature activity of single-component Pd-NP-based catalysts for the dehydrogenation of FA without sacrificial additives are still rare.

Support effects can be exploited to improve the catalytic performance of metal NPs in various catalytic reactions to a great extent.[9] Typical catalyst supports or stabilizers, including metal oxides,[8] activated carbon materials,[3] and metal–organic frameworks,[10] have been used to stabilize ultrafine Pd NPs to obtain more effective heterogeneous catalysts for the dehydrogenation of FA. However, the activities of previously described catalysts based on single-component Pd NPs are not yet sufficient. In the case of homogeneous metal-complex catalysts, the introduction of particular organic ligands enriches the electron density of metal active sites and thus enhances their activity for hydrogen generation.[2] In principle, it is also possible to enhance the catalytic activity of the nanoparticles in heterogeneous catalysts by the electron enrichment of Pd NPs. Nevertheless, effective approaches for tuning the electron density of Pd particles at the nanoscale have rarely been reported. On the other hand, noble-metal NPs have been widely used as cocatalysts to collect photogenerated electrons from photocatalysts (usually semiconductors) and enable the reduction of water with an increased rate of H_2 evolution.[11] However, current efforts are mainly focused on electron- and hole-induced redox reactions.[12] It is thus of great interest to investigate the possibility of applying Mott–Schottky catalysis to enhance the catalytic activity of electron-enriched Pd NPs for other important organic reactions, for example, the dehydrogenation of FA.

For the construction of effective Mott–Schottky catalysts based on Pd NPs, a rectifying contact between the Pd NPs and the semiconductive support is required; this contact depends on the band structure of the semiconducting material.[13] Among the semiconductors available for the embedding of metal NPs, nanostructured carbon nitride (g-C_3N_4, also abbreviated as CN)[14] with a band gap of 2.7 eV has proved to be an ideal candidate, as the work function of most noble metals is located between the conduction band and the valence band of g-C_3N_4.[11a,12d] As shown in Figure 1 A, metal NPs (exemplified by Pd herein) with higher work functions can give rise to an elevated Schottky barrier and thus enhance the charge separation at the contacted interface of the NP and g-C_3N_4. Moreover, cheap, abundant, and stable nanostructured g-C_3N_4 with rich in-built amino surface functional groups outperforms its inorganic semiconductive counterparts in stabilizing various metal NPs.[12d]

Herein, we report the application of the Mott–Schottky catalyst based on Pd NPs and g-C_3N_4 (Pd@CN) in the room-temperature dehydrogenation of FA in water. Simply through the construction of the rectifying contact between Pd NPs and graphitic carbon nitride, the rate of evolution of hydrogen gas over the catalyst (Pd@CN) at room temperature is elevated

---

[*] Y. Y. Cai, Prof. X. H. Li, Y. N. Zhang, Dr. X. Wei, Prof. K. X. Wang, Prof. J. S. Chen
School of Chemistry and Chemical Engineering
Shanghai Jiao Tong University
Shanghai 200240 (P. R. China)
E-mail: xinhaoli@sjtu.edu.cn
chemcj@sjtu.edu.cn

[**] This research was supported by the National Basic Research Program of China (2013CB934102, 2011CB808703) and the National Natural Science Foundation of China.

Supporting information for this article is available on the WWW under http://dx.doi.org/10.1002/anie.201304652.

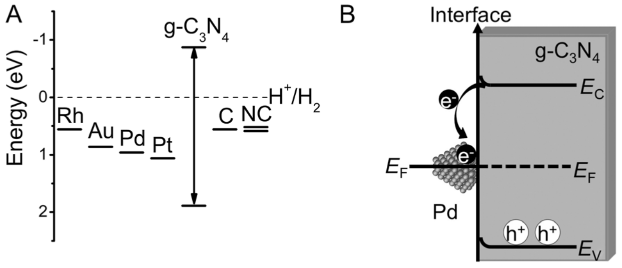

Figure 1. A) Work functions of typical metals and carbon, and band structures of carbon nitride and N-doped carbon (NC). B) Schematic view of a Mott–Schottky-type Pd@CN contact (E_F: work function; E_C: conduction band; E_V: valence band).

markedly as compared with that in the presence of the benchmark catalyst, carbon-supported Pd NPs. The activity of Pd@CN as a photocatalyst can be further enhanced through irradiation with visible light.

Mott–Schottky type Pd@CN catalysts with mesoporous carbon nitride as the catalyst support were fabricated by conventional wet impregnation (see the Supporting Information for details). Since soluble polymer molecules and organic ligands can form an insulating layer between Pd and carbon nitride that is not favorable for the rectifying contact, organic stabilizers were not involved in our synthetic process. Control samples with different catalyst supports, including nitrogen-doped layered carbon (N-LC, surface area: $190\,m^2g^{-1}$)[15] and carbon black (CB, surface area: $80\,m^2g^{-1}$), were prepared under the same conditions as used for Pd@CN; the resulting materials are represented by Pd@N-LC and Pd@CB, respectively (for detailed information, see Table S1 in the Supporting Information). The weight percentage of the Pd NPs deposited on the mesoporous carbon nitride and the carbon materials was 8% in all cases. The powder X-ray diffraction (PXRD) patterns (see Figure S1 in the Supporting Information) of Pd@CN and Pd@N-LC exhibited broad Pd (111) peaks, which indicated the formation of Pd NPs with small sizes, whereas the sharp peaks of Pd (111), (200), and (220) in the PXRD pattern of Pd@CB suggested that the Pd NPs in this material were larger. X-ray photoelectron spectroscopy (XPS; see Figure S2) of all samples at the Pd 3d level unambiguously revealed the formation of metallic palladium on the surface of the catalyst supports. The average size of the Pd NPs in Pd@CN and Pd@N-LC were estimated to be 3–5 nm on the basis of analysis by transmission electron microscopy (TEM; see Figure S3). When graphitic carbon (exemplified herein by CB) was used as the catalyst support, the size of Pd NPs formed in situ was as large as 10 nm.

Considering the potential applications of FA as an H_2-storage medium for practical devices (e.g. fuel cells), a sustainable and cost-effective strategy for the release of H_2 from water solution of FA requires room-temperature dehydrogenation reactions without the involvement of sacrificial additives. To this end, we tested the activity of the Pd-NP-based catalysts for the decomposition of formic acid (1M) in water at room temperature. The Pd@CN sample exhibited the highest activity for the generation of H_2 gas with a TOF of $49.8\,mol\,H_2\,mol^{-1}\,Pd\,h^{-1}$ at 288 K (Figure 2). This excellent TOF value is more than six times higher than those (2.3 and 6.7) of the carbon-supported Pd catalysts (Pd@N-LC and Pd@CB) under the same conditions and is comparable to those of the best catalysts at higher temperatures (usually >350 K). It is also distinctly higher than those of previously reported single-component Pd-NP-based catalysts under similar conditions (see Table S2). As the surface area, types of nitrogen functional groups,[15] sizes of the Pd NPs, and Pd loadings (8 wt%) of Pd@CN and Pd@N-LC were similar (see Table S1), the highly enhanced catalytic activity of Pd@CN is attributed to the support effect, that is, the Mott–Schottky effect.

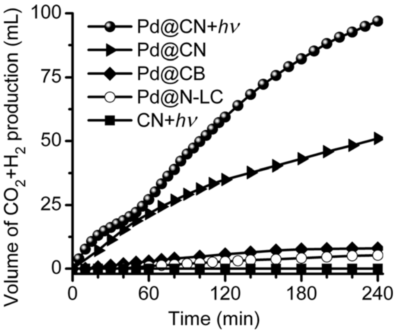

Figure 2. Decomposition of FA over different catalysts (CN: carbon nitride; CB: carbon black; N-LC: layered carbon; $h\nu$: irradiation with visible light ($\lambda \geq 400$ nm)). Typical conditions: 1 M aqueous FA solution (10 mL), Pd@CN-8% (20 mg), 288 K.

The Mott–Schottky effect is revealed by the remarkably decreased photoluminescence intensity (see Figure S4) of carbon nitride after the introduction of Pd NPs. For a Mott–Schottky heterojunction to be formed, electrons flow through the metal–semiconductor interface until the Fermi level equilibrium is reached, which results in bending of the conduction band (Figure 1B).[13] Indeed, the conduction-band position of carbon nitride is clearly lowered by coupling with Pd NPs, as confirmed by electrochemical analysis (see Figure S5).[14] Meanwhile, the band gap of carbon nitride remains nearly the same (see Figure S6). All these observations demonstrate the formation of a Mott–Schottky heterojunction at the interface of carbon nitride and the Pd NPs.

Visible light can be used to further promote the catalytic performance of Pd@CN for the dehydrogenation of FA (Figure 2), although the Mott–Schottky effect exists at the interface of Pd and g-C$_3$N$_4$ regardless of whether there is irradiation with light or not. The TOF was elevated to $71\,mol\,H_2\,mol^{-1}\,Pd\,h^{-1}$ at 288 K (reaction time: 2 h) under photoirradiation ($\lambda \geq 400$ nm). This TOF value surpassed all those of reported heterogeneous catalysts containing single-component Pd NPs for the dehydrogenation of FA under similar conditions (see Table S2). The Mott–Schottky effect can extend the lifetime of photogenerated charge carriers by enhancing charge separation at the interface. The decreased photoluminescence intensity (see Figure S4) and the increased photovoltage intensity (see Figure S6) of the Pd@CN sample as compared with those of bare CN unambiguously demonstrated the enhanced charge separation at the metal–semiconductor interface. The dehydrogenation reaction of formic acid did not consume electrons and holes. Moreover, visible-light irradiation was not effective at all in triggering the decomposition of FA over bare carbon nitride (squares, Figure 2). The only way that light can change the activity of Pd@CN is to enhance the electron enrichment of Pd NPs (Figure 3, inset). The Schottky barrier can prevent the reverse electron flow from the metal to the semiconductor; the electron enrichment of Pd NPs is thus facilitated when more electron–hole pairs are separated at the Mott–Schottky interface under photoirradiation. The effect of increased electron enrichment of the Pd NPs was further reflected by the significantly enhanced catalytic activity, whereas the structure, composition, and surface functional groups of the catalyst support (g-C_3N_4) remained the same before and after photoirradiation. More importantly, the enhanced catalytic performance of the Mott–Schottky catalyst is wavelength-dependent (Figure 3). These results directly demonstrate the key role of the Mott–Schottky effect in promoting the catalytic activity of Pd@CN.

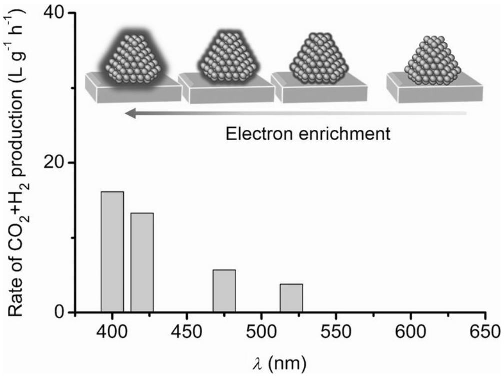

Figure 3. Dependence of the activity of Pd@CN on the irradiation wavelength for the photocatalytic decomposition of FA. Reaction conditions: 1 M aqueous FA solution (10 mL), Pd@CN-1 % (20 mg), 1 h, 288 K.

A dehydration reaction might also occur in the decomposition of FA. Such a reaction would result in the release of CO, which is unwanted for practical applications. A base trap containing 10 M NaOH was used to remove CO_2 from the as-formed gas of the catalytic reaction, and a loss of around 50 % in volume was observed (see Figure S7). No CO was detected in either the as-formed or the base-treated gas phase by IR spectroscopy (see Figure S8). Analysis by gas chromatography (GC; see Figure S9) further confirmed that the gas treated with the base trap was pure hydrogen with no CO and thus excluded the possibility of a dehydration reaction over Pd@CN in the current catalytic system. Therefore, the decomposition of FA over the Mott–Schottky catalyst proceeds only through a dehydrogenation pathway.

Besides the support effect, the content of Pd NPs in the catalyst also affects the catalytic performance. Pd@CN with weight percentages of Pd from 1 to 17 % (Pd@CN-x %, $x = 1$–17) were prepared under the same conditions. The sizes of the Pd NPs in Pd@CN-x % were all around 4 nm (see Figure S10), which excludes a possible size effect of Pd NPs on their catalytic activity. The volume of gas ($CO_2 + H_2$) generated in the dehydrogenation of a 1 M aqueous solution of FA (10 mL) was plotted against the reaction time over the Pd@CN-x % catalysts (20 mg) at 288 K with and without photoirradiation (see Figure S11). The rate of gas evolution generally increased as the weight percentage of Pd increased up to 8 %, as more active sites for the dehydrogenation of FA were introduced on the surface of g-C_3N_4. Since the surface active sites for the construction of rectifying Mott–Schottky contacts are limited, and too much Pd (> 10 %, Figure 4 A) might partially block the active sites, Pd@CN-8 % is the optimum catalyst for maximizing the Mott–Schottky effect in promoting gas evolution.

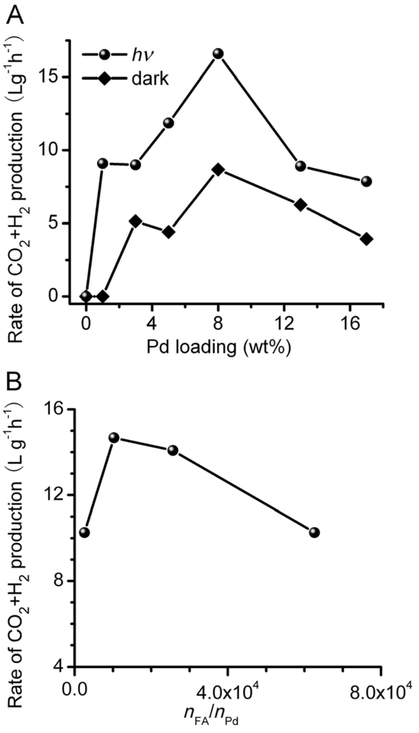

Figure 4. Effect of A) the Pd loading (conditions: 1 M aqueous FA solution (10 mL), catalyst (20 mg), 4 h, 288 K) and B) the molecular ratio of FA and Pd (conditions: 1 M aqueous FA solution (10 mL), catalyst (5–123 mg), 4 h, 288 K) on the mean gas-evolution rate in the dehydrogenation of FA with (spheres) and without photoirradiation ($\lambda \geq 400$ nm; diamonds).

To determine the effect of the molecular ratio of FA (n_{FA}) to Pd (n_{Pd}) on the catalytic performance of Pd@CN, various amounts of the best catalyst, Pd@CN-8 %, were used to catalyze the dehydrogenation of a 1 M aqueous FA solution (10 mL) at 288 K. For heterogeneous catalytic reactions, the reaction rate depends principally on mass transfer or diffusion between the liquid phase and the solid phase (in this case, the catalyst).[16] Considering the fixed concentration and thus the unchanged diffusion rate of FA in these experiments, the amount of the solid catalyst dominates the reaction rate. When 122 mg of Pd@CN-8 % was used, the conversion of FA reached 100 % within 300 min (see Figure S12), although the reaction rate was low. The conversion of FA decreased as the amount of Pd@CN-8% decreased. An $n_{\mathrm{FA}}/n_{\mathrm{Pd}}$ ratio of approximately 10000 (20 mg of Pd@CN-8% for 10 mL of a 1 M solution of FA) offered the highest gas-generation rate within 4 h (Figure 4B), thus revealing the mass-transfer-dependent activity of the Pd@CN catalyst.[16]

We further investigated the stability and reusability of the Pd@CN catalyst for practical applications. There was only a slight decrease in the activity of the reused Pd@CN catalyst when a certain amount of FA was added every 90 min to keep the concentration of FA around 1 M (see Figure S13). This deactivation is mainly attributed to the slightly increased particle size (5 nm) of the Pd NPs (see Figure S14B) and the corresponding decrease in the amount of active sites for the dehydrogenation of FA. At the end of the reaction, the catalyst support remained unchanged as a result of its high chemical stability (see Figure S14A, inset). More importantly, the Pd@CN catalyst can even be used in pure FA (98%) for the dehydrogenation reaction (see Figure S15): an indication of the great potential of these catalysts for practical large-scale and sustainable applications.

In conclusion, we have introduced the application of a Mott–Schottky catalyst to significantly promote the activity of Pd NPs for the dehydrogenation of FA in a sustainable manner. Under similar operating conditions, the catalytic performance of Pd@CN was found to be orders of magnitudes higher than that of similar Pd@carbon catalysts. A nanostructured carbon nitride acted as both the stabilizer and semiconductive support for the coupling of metal NPs to form the required rectifying Mott–Schottky nanoheterojunctions. This study suggests a general approach for further improvement of the catalytic performance of various metal NPs. In combination with the current success in fabricating excellent catalysts (e.g. multiple-component metal NPs), further engineering of the electronic structure of metal–NPs@CN dyads should generate new possibilities for the development of more efficient and sustainable catalysts for green energy systems.

Received: May 29, 2013

Keywords: heterogeneous catalysis · hydrogen generation · Mott–Schottky catalysts · nanostructures · photocatalysis

---

[1] a) K. Sekizawa, K. Maeda, K. Domen, K. Koike, O. Ishitani, *J. Am. Chem. Soc.* **2013**, *135*, 4596; b) D. Preti, S. Squarcialupi, G. Fachinetti, *Angew. Chem.* **2010**, *122*, 2635; *Angew. Chem. Int. Ed.* **2010**, *49*, 2581; c) J. F. Hull, Y. Himeda, W.-H. Wang, B. Hashiguchi, R. Periana, D. J. Szalda, J. T. Muckerman, E. Fujita, *Nat. Chem.* **2012**, *4*, 383; d) A. Boddien, F. Gärtner, C. Federsel, P. Sponholz, D. Mellmann, R. Jackstell, H. Junge, M. Beller, *Angew. Chem.* **2011**, *123*, 6535; *Angew. Chem. Int. Ed.* **2011**, *50*, 6411; e) T. Schaub, R. A. Paciello, *Angew. Chem.* **2011**, *123*, 7416; *Angew. Chem. Int. Ed.* **2011**, *50*, 7278; f) H. Kobayashi, M. Yamauchi, H. Kitagawa, Y. Kubota, K. Kato, M. Takata, *J. Am. Chem. Soc.* **2008**, *130*, 1828.

[2] a) S. Fukuzumi, T. Kobayashi, T. Suenobu, *J. Am. Chem. Soc.* **2010**, *132*, 1496; b) A. Boddien, B. Loges, F. Gärtner, C. Torborg, K. Fumino, H. Junge, R. Ludwig, M. Beller, *J. Am. Chem. Soc.* **2010**, *132*, 8924; c) A. Boddien, D. Mellmann, F. Gärtner, R. Jackstell, H. Junge, P. J. Dyson, G. Laurenczy, R. Ludwig, M. Beller, *Science* **2011**, *333*, 1733.

[3] Z.-L. Wang, J.-M. Yan, H.-L. Wang, Y. Ping, Q. Jiang, *Sci. Rep.* **2012**, *2*, 598.

[4] Q. Luo, G. Feng, M. Beller, H. Jiao, *J. Phys. Chem. C* **2012**, *116*, 4149.

[5] a) X. Zhou, Y. Huang, W. Xing, C. Liu, J. Liao, T. Lu, *Chem. Commun.* **2008**, 3540; b) S. Zhang, Ö. Metin, D. Su, S. Sun, *Angew. Chem.* **2013**, *125*, 3769; *Angew. Chem. Int. Ed.* **2013**, *52*, 3681; c) Ö. Metin, X. Sun, S. Sun, *Nanoscale* **2013**, *5*, 910.

[6] Z.-L. Wang, J.-M. Yan, Y. Ping, H.-L. Wang, W.-T. Zheng, Q. Jiang, *Angew. Chem.* **2013**, *125*, 4502; *Angew. Chem. Int. Ed.* **2013**, *52*, 4406.

[7] K. Tedsree, T. Li, S. Jones, C. W. A. Chan, K. M. K. Yu, P. A. J. Bagot, E. A. Marquis, G. D. W. Smith, S. C. E. Tsang, *Nat. Nanotechnol.* **2011**, *6*, 302.

[8] Q.-Y. Bi, X.-L. Du, Y.-M. Liu, Y. Cao, H.-Y. He, K.-N. Fan, *J. Am. Chem. Soc.* **2012**, *134*, 8926.

[9] a) Y. Wang, J. Yao, H. Li, D. Su, M. Antonietti, *J. Am. Chem. Soc.* **2011**, *133*, 2362; b) K. K. R. Datta, B. V. S. Reddy, K. Ariga, A. Vinu, *Angew. Chem.* **2010**, *122*, 6097; *Angew. Chem. Int. Ed.* **2010**, *49*, 5961; c) Y. Wan, H. Wang, Q. Zhao, M. Klingstedt, O. Terasaki, D. Zhao, *J. Am. Chem. Soc.* **2009**, *131*, 4541; d) R. Liu, S. M. Mahurin, C. Li, R. R. Unocic, J. C. Idrobo, H. Gao, S. J. Pennycook, S. Dai, *Angew. Chem.* **2011**, *123*, 6931; *Angew. Chem. Int. Ed.* **2011**, *50*, 6799.

[10] X. Gu, Z.-H. Lu, H.-L. Jiang, K. Akita, Q. Xu, *J. Am. Chem. Soc.* **2011**, *133*, 11822.

[11] a) X. C. Wang, K. Maeda, A. Thomas, K. Takanabe, G. Xin, J. M. Carlsson, K. Domen, M. Antonietti, *Nat. Mater.* **2009**, *8*, 76; b) X. H. Li, J. S. Zhang, X. F. Chen, A. Fischer, A. Thomas, M. Antonietti, X. C. Wang, *Chem. Mater.* **2011**, *23*, 4344.

[12] a) S. Linic, P. Christopher, D. B. Ingram, *Nat. Mater.* **2011**, *10*, 911; b) C. H. Dai, J. M. R. Narayanam, C. R. J. Stephenson, *Nat. Chem.* **2011**, *3*, 140; c) L. Li, G.-D. Li, C. Yan, X.-Y. Mu, X.-L. Pan, X.-X. Zou, K.-X. Wang, J.-S. Chen, *Angew. Chem.* **2011**, *123*, 8449; *Angew. Chem. Int. Ed.* **2011**, *50*, 8299; d) X. H. Li, X. C. Wang, M. Antonietti, *Chem. Sci.* **2012**, *3*, 2170; e) X. H. Li, M. Baar, S. Blechert, M. Antonietti, *Sci. Rep.* **2013**, *3*, 1743; f) X. H. Li, M. Antonietti, *Chem. Soc. Rev.* **2013**, *42*, 6593.

[13] a) G. L. J. A. Rikken, D. Braun, E. G. J. Staring, R. Demandt, *Appl. Phys. Lett.* **1994**, *65*, 219; b) V. Subramanian, E. Wolf, P. V. Kamat, *J. Phys. Chem. B* **2001**, *105*, 11439; c) V. Subramanian, E. Wolf, P. V. Kamat, *J. Am. Chem. Soc.* **2004**, *126*, 4943; d) T. Hirakawa, P. V. Kamat, *J. Am. Chem. Soc.* **2005**, *127*, 3928; e) X. H. Li, J. S. Chen, X. C. Wang, J. H. Sun, M. Antonietti, *J. Am. Chem. Soc.* **2011**, *133*, 8074.

[14] L. Kronik, Y. Shapira, *Surf. Sci. Rep.* **1999**, *37*, 1.

[15] X. H. Li, S. Kurasch, U. Kaiser, M. Antonietti, *Angew. Chem.* **2012**, *124*, 9827; *Angew. Chem. Int. Ed.* **2012**, *51*, 9689.

[16] R. Klaewkla, M. Arend, W. F. Hoelderich, *Mass Transfer—Advanced Aspects* (Ed.: H. Nakajima), InTech, http://www.intechopen.com/books/mostdownloaded/mass-transfer-advanced-aspects, **2011**, p. 636.